

Constant circulation sequences of binary neutron stars and their spin characterization

Antonios Tsokaros,¹ Kōji Uryū,² Milton Ruiz,¹ and Stuart L. Shapiro^{1,3}

¹*Department of Physics, University of Illinois at Urbana-Champaign, Urbana, Illinois 61801*

²*Department of Physics, University of the Ryukyus, Senbaru, Nishihara, Okinawa 903-0213, Japan*

³*Department of Astronomy & NCSA, University of Illinois at Urbana-Champaign, Urbana, Illinois 61801*

(Dated: January 1, 2019)

For isentropic fluids, dynamical evolution of a binary system conserves the baryonic mass and circulation; therefore, sequences of constant rest mass and constant circulation are of particular importance. In this work, we present the extension of our Compact Object CALCulator (COCAL) code to compute such quasiequilibria and compare them with the well-known corotating and irrotational sequences, the latter being the simplest, zero-circulation case. The circulation as a measure of the spin for a neutron star in a binary system has the advantage of being exactly calculable since it is a local quantity. To assess the different measures of spin, such as the angular velocity of the star, the quasilocal, dimensionless spin parameter J/M^2 , or the circulation \mathcal{C} , we first compute sequences of single, uniformly rotating stars and describe how the different spin diagnostics are related to each other. The connection to spinning binary systems is accomplished through the concept of circulation and the use of the constant rotational velocity formulation. Finally, we explore a modification of the latter formulation that naturally leads to differentially rotating binary systems.

I. INTRODUCTION

Some of the most important problems in modern astrophysics include: a) the origin of the heavy elements in the periodic table (heavier than iron), b) the behavior of matter at densities beyond the nuclear, and c) the mechanism behind the powerful electromagnetic events known as gamma-ray bursts, which in a few seconds release as much energy as the sun does throughout its entire life. The extreme conditions necessary for the creation of these phenomena can be found in a binary neutron star (BNS) system through the combination of immense gravity, electromagnetic fields, and nuclear forces. The 2017 detection of GW170817 confirmed these hypotheses and marked the birth of “multimessenger astronomy” since for the first time gravitational waves from a BNS system were directly measured by the LIGO/VIRGO detector [1] together with a short duration gamma-ray burst by the Fermi Gamma-Ray Burst Monitor [2] and INTEGRAL [3].

One of the most important characteristics of a neutron star (NS) is its rotational frequency, which in isolation has been observed to be as high as 716 Hz, corresponding to a period of 1.4 ms for PSR J1748-2446ad [4]. In the 18 BNS systems currently known in the Galaxy [5, 6], the rotational frequencies are typically smaller. The NS in the system J1807-2500B has a period of 4.2 ms, while systems J1946+2052 [7], and J1757-1854 [8], J0737-3039A [9] have periods 16.96, 21.50, and 22.70 ms, respectively.

Any evolution simulation of a BNS starts from initial data that describe the system under consideration. The first such binary initial data were calculated by Baumgarte *et al.* [10, 11] and Marronetti *et al.* [12] and described two NSs tidally locked, as for example the Earth-Moon system. These were the so-called corotating solutions, and although they gave the first insight into the problem, they were rendered unrealistic since the viscosity is too small in NSs to achieve synchronization [13, 14]. A more realistic scenario is the so-called irrotational state where the two NSs have zero vorticity. Such systems were more difficult to describe and required an additional potential equation. Irrotational BNS systems using

different numerical methods were presented by Bonazzola *et al.* [15],ourgoulhon *et al.* [16], Marronetti *et al.* [17, 18], and Uryū *et al.* [19, 20]. Even today, the majority of the BNS simulations adopt these methods and therefore assume that the spin of the individual NSs is zero. Such an assumption, although adequate in most cases, cannot for example describe systems J1946+2052, J1757-1854, and J0737-3039A which, according to Ref. [6], will have periods at merger of 18.23, 27.09, and 27.17 ms, respectively. For accurate gravitational wave analysis, one cannot consider these binaries to be irrotational, and the spin of each NS must be taken into account. Also, event GW170817 [1] was unable to rule out high spin priors and thus two sets of data (for low and high spins) were consistent with the observations.

Going beyond the two extreme cases of corotating and irrotational BNSs and constructing binaries with arbitrary spin has proven to be more difficult due to the fact that the Euler equation does not yield a trivial integral. The first attempt to address that problem was by Marronetti and Shapiro [21], who used instead the Bernoulli equation (first integral along *flow lines* and not globally) to construct sequences of constant circulation. In Refs. [22, 23], Baumgarte and Shapiro presented an alternative formulation to compute arbitrary spinning binaries by constructing a new elliptic equation from the divergence of the Euler equation. Although no solutions were presented there, violations of the Euler equations were expected since their rotational part was not required to vanish. The only self-consistent formulation to obtain BNSs with arbitrary spinning initial data was presented by Tichy [24], and quasiequilibrium sequences were computed in Ref. [25]. In these studies, a first integral of the fluid flow was obtained under suitable assumptions, and binary sequences with approximately constant rotational velocity of each component were calculated. From a different perspective, Tsatsin and Marronetti [26] presented a method to produce initial data for spinning BNSs that allowed for arbitrary orbital and radial velocities, but without satisfying the Hamiltonian and momentum constraints.

In this work, we present the extension of our Compact Ob-

ject CALculator (COCAL) code for BNSs [27–29] to compute quasidequilibrium binary sequences of constant rest mass and circulation. For isentropic fluids, dynamical evolution of a binary system conserves the baryonic mass and circulation; therefore, sequences that conserve these quantities can be considered realistic “snapshots” of an evolutionary scenario. We use Tichy’s spinning formulation [24] as we did in Ref. [28], where sequences of constant rest mass alone were computed, but focus here on the different spin measures that are currently used [30–32] in order to make a critical assessment. Using the circulation and rest mass as fundamental properties, a connection between spinning companions in binaries and single axisymmetric stars is established, and differences are discussed. Finally, we present a decomposition alternative to Ref. [24], which slightly simplifies the equations to be solved and leads naturally to differentially rotating binary systems. Binary sequences of that kind are computed and compared with the ones coming from the original formulation [24].

In this paper, spacetime indices are greek, spatial indices are latin, and the metric signature is $-+++$. For writing the basic equations, geometric units with $G = c = 1$ are used, while in all numerical solutions, $G = c = M_\odot = 1$ units are used for convenience.

II. EQUATIONS AND GENERAL ASSUMPTIONS

According to the first law of thermodynamics for binary systems by Friedman *et al.* [33, 34], if one assumes a spatial geometry Σ_t that is conformally flat, neighboring equilibria of asymptotically flat spacetimes with a helical Killing vector asymptotic form $k^\alpha = t^\alpha + \Omega\phi^\alpha$ (t^α and satisfy

$$\delta M = \Omega\delta J + \int_{\Sigma_t} [\bar{T}\Delta dS + \bar{\mu}\Delta dM_B + V^\alpha\Delta dC_\alpha] + \sum_i \frac{1}{8\pi} \kappa_i \delta A_i. \quad (1)$$

Here, M and J are the Arnowitt-Deser-Misner (ADM) mass and angular momentum of the spacetime, while Ω is the orbital angular velocity; \bar{T} and $\bar{\mu}$ are the redshifted temperature and chemical potential; dM_B is the baryon mass of a fluid element; dC_α is related to the circulation of a fluid element and V^α is the velocity with respect to the corotating frame; and κ_i and A_i are the surface gravity and the areas of black holes. For isentropic fluids, dynamical evolution conserves the baryon mass, entropy, and vorticity of each fluid element, and thus the first law yields $\delta M = \Omega\delta J$. Equation (1) implies that a natural measure to characterize the spin of a NS in a binary setting is its circulation in a manner similar to the way rest mass characterizes the mass. Since different spin measures are used in BNS studies [30–32], one question that arises is how all these diagnostics are related to the conserved quantity of circulation. Before answering this question we will investigate the relationship of these quantities for single, axisymmetric, rotating stars. We will adopt the 3+1 formulation of [35] in order to make contact with the theory of a single rotating star, while for BNS systems, we will use the notation

of Ref. [28]. The equations solved are reported in detail in those two papers, so here we will only review the necessary definitions and assumptions in a unified way.

We assume that the spacetime \mathcal{M} is asymptotically flat and is foliated by a family of spacelike hypersurfaces $(\Sigma_t)_{t \in \mathbb{R}}$, parametrized by a time coordinate $t \in \mathbb{R}$ as $\mathcal{M} = \mathbb{R} \times \Sigma_t$ [36]. The future-pointing unit normal one form to Σ_t , $n_\alpha := -\alpha\nabla_\alpha t$, is related to the generator of time translations t^α as $t^\alpha := \alpha n^\alpha + \beta^\alpha$, where $t^\alpha\nabla_\alpha t = 1$. α and β^α are, respectively, the lapse and shift and β^α is spatial, $\beta^\alpha\nabla_\alpha t = 0$. The projection tensor to Σ_t γ_α^β is introduced as $\gamma_\alpha^\beta := g_\alpha^\beta + n^\alpha n_\beta$. The induced spatial metric γ_{ab} on Σ_t is the projection tensor restricted to it. Introducing a conformal factor ψ , and a conformally rescaled spatial metric $\tilde{\gamma}_{ab}$, the line element on a chart $\{t, x^i\}$ of Σ_t is written as

$$ds^2 = -\alpha^2 dt^2 + \psi^4 \tilde{\gamma}_{ij} (dx^i + \beta^i dt)(dx^j + \beta^j dt). \quad (2)$$

The conformal rescaling is determined from a condition $\tilde{\gamma} = f$, where $\tilde{\gamma}$ and f are determinants of the rescaled spatial metric $\tilde{\gamma}_{ab}$ and the flat metric f_{ab} . In what follows, we will assume that $\tilde{\gamma}_{ij} = f_{ij}$ for both single and binary star computations.

The extrinsic curvature of each slice Σ_t is defined by

$$\begin{aligned} K_{ab} &:= -\frac{1}{2}\gamma^\alpha_a \gamma^\beta_b \mathcal{L}_n \gamma_{\alpha\beta}, \\ &= -\frac{1}{2\alpha} \partial_t \gamma_{ab} + \frac{1}{2\alpha} \mathcal{L}_\beta \gamma_{ab}, \end{aligned} \quad (3)$$

where $\partial_t \gamma_{ab}$ is the pullback of $\mathcal{L}_t \gamma_{\alpha\beta}$ to Σ_t , \mathcal{L}_t is the Lie derivative along the vector t^α defined on \mathcal{M} , and \mathcal{L}_β is the Lie derivative along the spatial vector β^a on Σ_t . Hereafter, we denote the trace of K_{ab} by K , and the trace-free part of K_{ab} by $A_{ab} := K_{ab} - \frac{1}{3}\gamma_{ab}K$. For both single and BNS systems we will assume the maximal slicing condition

$$K = 0. \quad (4)$$

In this paper, we consider perfect-fluid spacetimes in which the stress-energy tensor is written as [28]

$$T^{\alpha\beta} := (\epsilon + p)u^\alpha u^\beta + pg^{\alpha\beta}, \quad (5)$$

where ϵ is the energy density, p is the pressure, and u^α is the 4-velocity. The relativistic enthalpy h is defined as

$$h := \frac{\epsilon + p}{\rho}, \quad (6)$$

where ρ is the rest mass density. The 4-velocity of the fluid can be written as $u^\alpha = u^t(1, v^i)$ and, in analogy to a Newtonian decomposition, we can split the spatial component v^i into two parts: one that follows the rotation around the center of mass, $\Omega\phi^i$, and one that represents the velocity in the corotating frame V^i ,

$$u^\alpha := u^t(t^\alpha + v^\alpha) = u^t(k^\alpha + V^\alpha), \quad (7)$$

where $v^\alpha = (0, v^i) := \Omega\phi^\alpha + V^\alpha$, and

$$k^\alpha := t^\alpha + \Omega\phi^\alpha = \alpha n^\alpha + \omega^\alpha. \quad (8)$$

Here, the helical Killing vector k^α applies to either a binary system having orbital angular velocity Ω or a single rotating star (axisymmetric or not) having the same constant, rotating angular velocity. The vector $\omega^\alpha := \beta^\alpha + \Omega\phi^\alpha$ is the so-called corotating shift. For single rotating stars as well as for corotating binaries, $V^\alpha = 0$.

Fluid variables will be computed through the conservation of the energy-momentum tensor

$$\begin{aligned} 0 &= \nabla_\alpha T^\alpha_\beta \\ &= \rho[u^\alpha \nabla_\alpha (hu_\beta) + \nabla_\beta h - T\nabla_\beta s] + hu_\beta \nabla_\alpha (\rho u^\alpha) \\ &= \rho[u^\alpha \omega_{\alpha\beta} - T\nabla_\beta s] + hu_\beta \nabla_\alpha (\rho u^\alpha), \end{aligned} \quad (9)$$

and local conservation of rest mass

$$\nabla_\alpha (\rho u^\alpha) = 0. \quad (10)$$

Assuming isentropic configurations, the relativistic Euler equation becomes $u^\alpha \omega_{\alpha\beta} = 0$, where

$$\omega_{\alpha\beta} := \nabla_\alpha (hu_\beta) - \nabla_\beta (hu_\alpha) \quad (11)$$

is the relativistic vorticity tensor, which is zero for irrotational flow [37].

In 3+1 language, the Euler equation and the rest mass conservation equation become [28]

$$\gamma_i^\alpha \mathcal{L}_k (hu_\alpha) + D_i \left(\frac{h}{u^t} + hu_j V^j \right) + V^j \omega_{ji} = 0, \quad (12)$$

$$\mathcal{L}_k (\rho u^t) + \frac{1}{\alpha} D_i (\alpha \rho u^t V^i) = 0, \quad (13)$$

where D is the covariant derivative with respect to the spatial metric, $D_\alpha \gamma_{ij} = 0$.

For single rotating stars, as well as for corotating binaries under the helical symmetry assumption, Eq. (13) is trivially satisfied, while the Euler equation results in a simple algebraic equation,

$$\frac{h}{u^t} = C, \quad (14)$$

where C is a constant to be determined and $u^t = 1/\sqrt{\alpha^2 - \omega_i \omega^i}$.

For irrotational binaries [38–41], we have $\omega_{\alpha\beta} = 0$, so the specific enthalpy current hu_α can be derived from a potential $hu_\alpha = \nabla_\alpha \Phi$. In order to allow for arbitrary spinning binary configurations, a 3-vector s^i is introduced according to [24]

$$\hat{u}_i := \gamma_i^\alpha hu_\alpha = D_i \Phi + s_i, \quad (15)$$

where the $D_i \Phi$ part corresponds to the ‘‘irrotational part’’ of the flow and s^i the ‘‘spinning part’’ of the flow. In our code vector s^i is the input quantity, and $s_i = \gamma_{ij} s^j$. For a general vector s^i , one can have a binary system that exhibits differential rotation. Irrotational binaries are recovered for $s^i = 0$. According to Ref. [25] a choice that minimizes differential rotation is a rigid rotation law,

$$s^i := \Omega_s^a \phi_s^i \quad (16)$$

where $\phi_s^{i(a)} = \epsilon^{iaj} X_j$ denotes the rotation vectors along the NS’s three axes. The index i corresponds to the component of the vector $\phi_s^{(a)}$, while the index inside the parenthesis names the three different vectors. Vector $\phi_s^{i(3)}$, which in the following sections is denoted by ϕ_s^i , is the rotation vector along the star’s X_3 -axis, in contrast to ϕ^i which is the rotation vector along the z -axis. For single rotating stars these two vectors are identical. We denote by $x_i = \{x, y, z\}$ the coordinates around the center of mass of the binary system, and by $X_a = \{X_1, X_2, X_3\}$ the coordinates centered at the maximum density point of each NS. The orbital vector ϕ^i refers to $\{x, y, z\}$ while the spin vector s^i refers to $\{X_1, X_2, X_3\}$. In this work we assume that the rotation of the neutron stars is around X_3 . The z -axis and the X_3 axis are parallel and perpendicular to the orbital plane. The coefficients Ω_s^a are parameters that control the rotational spin around the NS’s three axes X_a . These parameters, although lacking of physical (i.e. invariant) meaning, approximately represent the angular velocity of the rotating star.

From Eqs. (7) and (15), the spatial velocity V^i of the flow is

$$V^i = \frac{D^i \Phi + s^i}{hu^t} - \omega^i. \quad (17)$$

For arbitrary spinning binaries, the Euler equation (12) becomes

$$\gamma_i^\alpha [\mathcal{L}_k (hu_\alpha) + \mathcal{L}_V (s_\alpha)] + D_i \left(\frac{h}{u^t} + V^j D_j \Phi \right) = 0, \quad (18)$$

which under the assumptions of helical symmetry and the additional assumption of

$$\mathcal{L}_V (s_\alpha) = 0 \quad (19)$$

yields

$$\frac{h}{u^t} + V^j D_j \Phi = C, \quad (20)$$

where again C is a constant to be determined. Although the Euler integral has the same form for both irrotational and spinning binaries, it produces a different equation since the 3-velocity V^i is different in these two cases. Assumption (19) means that changes of the spin vector with respect to the corotating velocity are small.

The normalization condition $u_\alpha u^\alpha = -1$, together with Eqs. (15), (17), and (20), yield

$$hu^t = \frac{\lambda + \sqrt{\lambda^2 + 4\alpha^2 s_i (D^i \Phi + s^i)}}{2\alpha^2}, \quad (21)$$

$$h = \sqrt{\alpha^2 (hu^t)^2 - (D_i \Phi + s_i)(D^i \Phi + s^i)}. \quad (22)$$

Here, $\lambda := C + \omega^i D_i \Phi$. For purely irrotational binaries, $hu^t = \lambda/\alpha^2$ and $h = \sqrt{\lambda^2/\alpha^2 - D_i \Phi D^i \Phi}$. The fluid potential Φ is computed from the conservation of rest mass (13) and the use of Eqs. (20) and (17) [28].

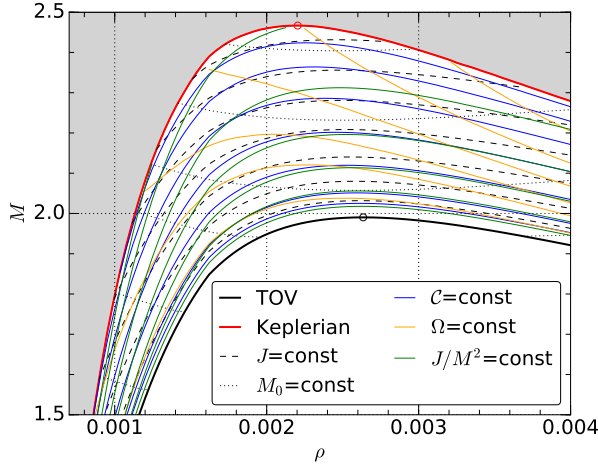


FIG. 1. Mass vs rest-mass density for sequences of uniformly rotating single stars with constant angular momentum J , rest mass M_0 , circulation \mathcal{C} , angular velocity Ω , dimensionless spin J/M^2 , together with the spherical (TOV) and mass-shedding (Kepler) limits.

III. MEASURES OF SPIN AND CONSTANT CIRCULATION SEQUENCES

A. Single stars

For single rotating stars, one has a variety of ways to characterize the spin. Among them are its angular velocity Ω (we assume constant rotation), its ADM angular momentum J

$$J = \frac{1}{8\pi} \int_{S_\infty} K^a_b \phi^b dS_a \quad (23)$$

or the dimensionless spin J/M^2 , where M is the ADM mass. Using Gauss's theorem, Eq. (23) can be written as

$$\begin{aligned} J &= \frac{1}{8\pi} \int_{V_t} D_a(K^a_b \phi^b) d\Sigma - \frac{1}{8\pi} \int_S K^a_b \phi^b dS_a \\ &= \frac{1}{8\pi} \int_{V_t} K^a_b \partial_a \phi^b d\Sigma - \frac{1}{8\pi} \int_S K^a_b \phi^b dS_a \end{aligned} \quad (24)$$

where $\partial V_t = S_\infty \cup S$. To go from the first volume integral to the second, we used the maximal slicing assumption and the momentum constraint with zero sources since S is taken to be outside the fluid volume. Without loss of generality, we can assume the S is a sphere just outside the surface of the NS.

When the conformal geometry is flat (as happens in most binary neutron star calculations), ϕ^a is a Killing vector of the conformal geometry, and therefore the volume integral in Eq. (24) is zero. We call the remain integral the quasilocal spin angular momentum

$$J_{\text{ql}} = \frac{1}{8\pi} \int_S K^a_b \phi^b dS_a \quad (25)$$

where here the unit normal is outward. Thus, under the assumptions of conformal flat geometry and maximal slicing,

$$J = J_{\text{ql}} \quad (\text{single stars}) . \quad (26)$$

Another way to measure the spin of a rotating star is by its circulation. For rotation around the z axis,

$$\mathcal{C} := \oint_c hu_\alpha dx^\alpha = \oint_c hu^t \psi^4 \delta_{ij} (\beta^i + \Omega \phi^i) dx^j , \quad (27)$$

where c can be taken to be a fluid equatorial ring. One of the advantages of using the circulation as a spin diagnostic is the fact that Eq. (27) is local in character and involves quantities that are exactly known (essentially the fluid velocity). Although all single rotating star models reported in this paper are axisymmetric, we have checked our circulation code in the case of single triaxial stars [35, 42], where the curve c is no longer a circle but close to an ellipse.

In order to understand how the different measures of spin are related to each other for single uniformly rotating stars, we use the COCAL code [35] to build sequences of constant angular momentum J , circulation \mathcal{C} , angular velocity Ω , and dimensionless spin J/M^2 , together with the spherical (TOV) and mass-shedding (Kepler) limits as in Fig. 1. For the equation of state (EoS), we have chosen the piecewise representation of ALF2 [43, 44], which according to event GW170817 it is still a viable choice. Having said that, we point out that the results of this work do not depend on this choice and any other EoS would have been as good for conveying the ideas we put forward here. In our code, we compute the circulation both as the line integral (27) and also as a surface integral using Stokes's theorem. Both quantities agree to the precision of our calculation, which is less than 1%. The curve c is chosen to be along the surface of the star in the xy plane, which, according to our normalization scheme (use of surface fitted coordinates), is the unit circle [35]. From the computational point of view, one important aspect of the COCAL code is the use of normalized coordinates for both single rotating stars [35] as well as binaries [28],

$$\hat{x}^i := \frac{x^i}{R_0}, \quad \hat{\Omega} := \Omega R_0 . \quad (28)$$

The normalization factor that determines the length scale R_0 is only found at the end of the iteration procedure and varies at every iteration. The constants R_0 , $\hat{\Omega}$, and C [from the hydrostatic equilibrium (14), (20)] are determined through a solution of a nonlinear 3×3 system as described in Refs. [28, 35].

In terms of the normalized quantities,

$$\mathcal{C} = R_0 \oint_c hu^t \psi^4 \delta_{ij} (\beta^i + \hat{\Omega} \hat{\phi}^i) d\hat{x}^j . \quad (29)$$

As one can see from Fig. 1, all curves that measure the spin of a rotating star are *in general distinct*. If a set of curves A is “parallel” to another set of curves B, this means that a star that is moving along a constant A sequence will also move along a constant B sequence, or in other words, conservation of quantity A will imply the conservation quantity B. As far as

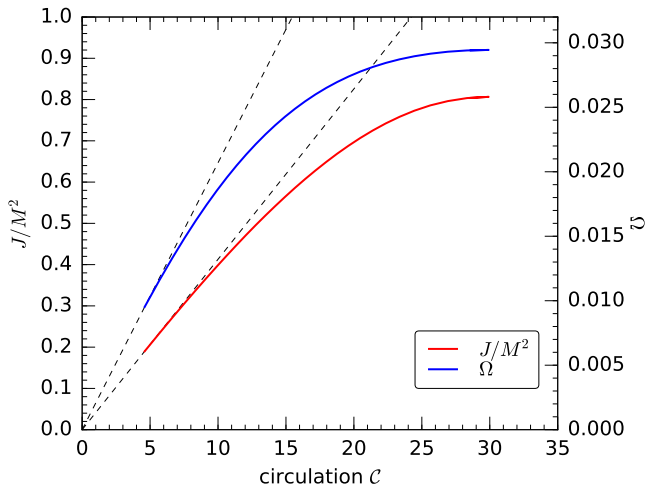


FIG. 2. Dimensionless spin parameter J/M^2 and angular velocity Ω vs circulation \mathcal{C} along a sequence of uniformly rotating, single stars with constant rest mass $M_0 = 1.5$.

the different spin measures $J, \Omega, \mathcal{C}, J/M^2$ for rotation close to the mass-shedding limit (red curve), this cannot happen since all sets of curves are distinctly different. By contrast, close to the spherical limit, one can see that constant circulation sequences are almost parallel to constant J/M^2 sequences. This means that the curve $\mathcal{C} = c_1$ will nearly coincide with a curve $J/M^2 = c_2$, (for two constants $c_1 \neq c_2$) when rotation is slow, and therefore if during a process one parameter is conserved, so is the other. In Fig. 2, we plot the dimensionless spin J/M^2 and angular velocity Ω vs the circulation for a sequence of constant rest mass $M_0 = 1.5$. Dashed black lines connect the first points of the sequences to the static limit (TOV). Along that sequence, the ADM mass varies approximately from 1.35 to 1.39. As we can see for dimensionless spins up to ~ 0.4 , the two quantities vary linearly, but for higher spins, especially close to the mass-shedding limit, this dependence becomes quadratic. Beyond this point, increasing the circulation results in a smaller increase in J/M^2 .

B. Binary stars

For a corotating binary, the circulation of each star is given by the same formula as in a single rotating star (27) where now the vector ϕ^i is the z-rotational vector (we assume the binary orbit to be in the xy-plane) around the center of mass. In Fig. 3's top panel, we plot the circulation \mathcal{C} and the ‘‘coordinate circulation’’ $\mathcal{C}_\beta := \oint_c h u^t \psi^4 \delta_{ij} \beta^i dx^j$ for a constant rest mass sequence with $M_0 = 1.5$ as a function of Ω . In the bottom panel, we plot the approximate coordinate equatorial area of each star $A \approx 2\pi R_x R_y$, normalized by its initial value in the sequence A_0 . As we can see, the circulation increases linearly with respect to the angular velocity, which provides yet another argument as to why the corotating state is not realistic for BNS systems with isentropic fluids. In the Newtonian

limit, $\mathcal{C} = 2A\Omega$, where A is the equatorial area of the NS. From the bottom panel of Fig. 3, we see that the equatorial area is approximately conserved along the sequence. Therefore, the circulation of the corotating sequence follows essentially the Newtonian law apart from a redshift factor. We also observe that, even when they are close to each other, the circulation of the corotating binaries is relatively small compared to the maximum circulation $\mathcal{C}_{\max} \approx 30$ for the ALF2 EoS for single rotating stars. From Fig. 2, this implies dimensionless spins lower than say ~ 0.4 (we calculate below the exact values). The coordinate circulation \mathcal{C}_β (green curve) has opposite sign from \mathcal{C} and typically grows also linearly and is $\sim 20\%$ of \mathcal{C} . For all binary calculations in this work, we used grid values as reported in Table I. In order to create binaries at different separations we choose $r_c \in \{1.125, 1.25, 1.50, 1.75\}$ where 1.125 leads to close binaries, while 1.75 to widely separated ones [28].

For an irrotational binary, the circulation is zero since the enthalpy current $h u_\alpha$ is a total derivative. For spinning binaries with 4-velocity (15) and spin along the orbital axis, the circulation becomes

$$\mathcal{C} = \oint_c s_i dx^i = R_0 \oint_c \psi^4 \delta_{ij} \hat{\Omega}_s \hat{\phi}_s^i dx^i, \quad (30)$$

where code (normalized) coordinates (28) are used. Here, $\Omega_s^a = (0, 0, \Omega_s)$ and $s^i := \Omega_s^3 \phi_s^i(3)$. Sequences of constant rest mass for fixed values of $\hat{\Omega}_s$ have been calculated in Ref. [28]. Here, we have extended our COCAL code [27, 28] in order to compute binary sequences of both constant circulation and rest mass. In order to do that, a multiroot secant method was implemented, which in principle can iterate over different quantities like densities, spins, or distances in order to achieve some target values. The computational cost, though, for such a finder increases considerably. In particular, the method converges after approximately ten cycles and for each cycle, one needs N_i converged solutions, where N_i is the number of quantities that we are targeting. For equal-mass binaries that we calculate here, in order to find a sequence of constant rest mass and circulation, ($N_i = 2$) ~ 20 converged solutions are needed. If one also insists these binary separations are at a certain distance (or angular velocity), then $N_i = 3$. For each converged solution, one needs ~ 500 iterations. Also in this work, we assume symmetric aligned or antialigned binaries; i.e. we only have to search for one out of the six spin components. For the general case, the computational cost will increase by an order of magnitude.

In Fig. 4, we plot the total angular momentum of the system for a sequence of constant circulation $\mathcal{C} = 4$, together with the familiar irrotational and corotating sequences. Also, the corresponding PN curves are plotted. The qualitative feature of a constant circulation curve is that it runs parallel to the irrotational curve at a higher angular momentum level for aligned spin binaries. This is not surprising since an irrotational curve has constant circulation $\mathcal{C} = 0$. Higher spinning binaries have curves shifted upward, and antialigned spinning binaries have curves parallel and below the level of the irrotational one. Another feature is that at large separations the constant circulation curve does not converge to the PN curves, which is also

Type	Patch	r_a	r_s	r_b	r_c	r_e	N_r^f	N_r^l	N_r^m	N_r	N_θ	N_ϕ	L
Hd2.0	COCP - 1	0.0	varies	10^2	varies	1.125	50	64	80	192	48	48	12
	COCP - 2	0.0	varies	10^2	varies	1.125	50	64	80	192	48	48	12
	ARCP	5.0	-	10^6	6.25	-	16	-	20	192	48	48	12

TABLE I. Grid structure parameters used for the binary computation in COCAL. r_a is the radial coordinate where the grids start, r_b the radial coordinate where the grids end, r_c the center-of-mass point (excised sphere is located at $2r_c$), r_e is the radius of the excised sphere, r_s is the radius of the sphere bounding the star's surface, N_r is the number of intervals Δr_i in $r \in [r_a, r_b]$, N_r^l is the number of intervals Δr_i in $r \in [0, 1]$, N_r^f is the number of intervals Δr_i in $r \in [0, r_s]$, N_r^m is the number of intervals Δr_i in $r \in [r_a, r_c]$, N_θ is the number of intervals $\Delta \theta_j$ in $\theta \in [0, \pi]$, N_ϕ is the number of intervals $\Delta \phi_k$ in $\phi \in [0, 2\pi]$, and L is the order of included multipoles. Distances are in normalized quantities, and r_s varies during the iterations in order for a specific distance (angular velocity) to be reached. For more details, see Refs. [27, 28].

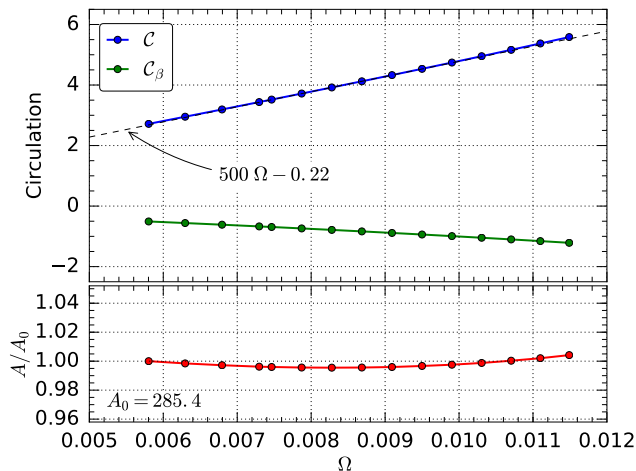


FIG. 3. The top panel shows circulation \mathcal{C} and coordinate circulation \mathcal{C}_β for a corotating BNS sequence of constant rest mass $M_0 = 1.5$. The bottom panel shows the approximate equatorial area $A \approx 2\pi R_x R_y$ of the each NS along the sequence. Values are normalized by A_0 , the area of the first member of the sequence.

expected since these binaries have spin angular momentum independent of the orbital angular momentum. That is also the reason why they intersect the corotating sequence curve which has small spin angular momentum at infinity and becomes larger as one moves toward smaller distances. Given the fact that a dynamical evolution conserves the rest mass, entropy, and circulation, a physical spinning sequence representing a merging binary is going to be like the red or blue one in Fig. 4. Points marked with a larger black circle denote the approximate innermost stable circular orbit (ISCO). Locating the ISCO is not essential for this work therefore its location as denoted in Figs. 4,5 can be further refined.

In Fig. 5, different spin measures are plotted along constant circulation sequences as well as a corotating one. $M_1 = 1.36$ corresponds to the ADM mass of a single star at infinity, and $J_{1,q1}$ corresponds to its quasilocal spin as calculated from Eq. (25) but with the rotational vector ϕ_s^i (which generates rotations around the star's center) instead of ϕ^i . J is the total angular momentum of the binary system, and J_{irr} is the-

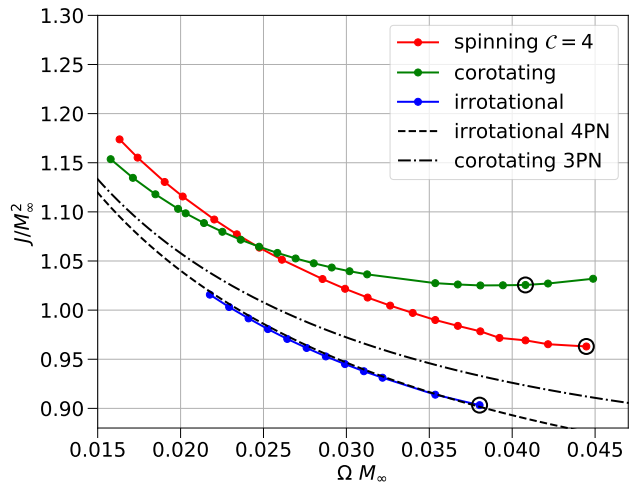


FIG. 4. Angular momentum curve for a binary sequence with constant circulation $\mathcal{C} = 4$ and rest mass $M_0 = 1.5$, along with the typical corotating and irrotational sequences of the same rest mass. Points marked with a larger black circle denote the approximate ISCO. Realistic physical sequences have constant circulation and rest mass, such as the red or blue one.

tal angular momentum of the irrotational binary at the same angular velocity. From the corotating (purple) sequence, one can see that the dimensionless spin $J_{1,q1}/M_1^2$ grows linearly as the separation decreases. Also even at very close separation (ISCO) this dimensionless spin is relatively small < 0.35 . This linear growth of the quasilocal spin is consistent with Figs. 2 (and 3), which also shows that behavior for small J/M^2 in single rotating stars. Sequences of constant circulation $\mathcal{C} = 4, 8$ are also plotted in Fig. 5. The curves (blue and red) show that within the accuracy of our computation the dimensionless quasilocal spin (or equivalently the quasilocal angular momentum) is also conserved along these sequences when the binaries are widely separated. As one moves towards the ISCO we observe a $\sim 10 - 15\%$ increase which is consistent with the increase found in evolutions [45]. This behavior is also consistent with Fig. 1, which shows that for slowly rotating single stars sequences of constant circulation are parallel to sequences of constant J/M^2 . Another mea-

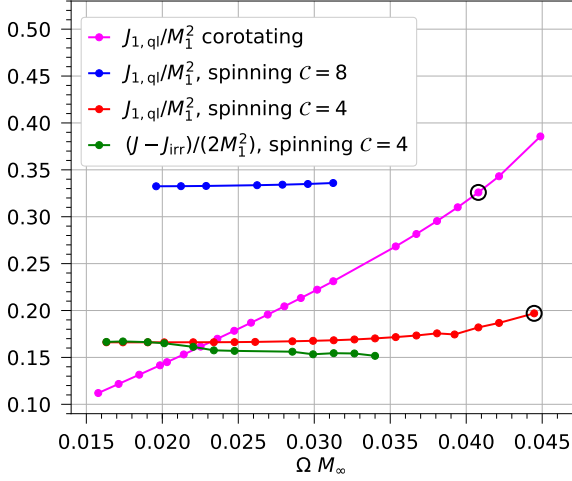


FIG. 5. Spin measures for an individual star in a binary setting. M_1 corresponds to the ADM mass of a single star at infinity, and $J_{1,q}$ corresponds to its quasilocal spin. Except for the green curve, all others show the quasilocal spin of a single star along a sequence. The green curve estimates the spin by comparison with an irrotational sequence at the same orbital angular velocity points. Points marked with a larger black circle denote the approximate ISCO.

sure of spin typically quoted in the literature is the difference between the angular momentum at infinity of the irrotational solution from the corresponding spinning solution. In Fig. 5, we plot this spin measure of the $C = 4$ sequence by comparing it with the corresponding irrotational sequence (green curve). The plot shows that, although at larger separations the two diagnostics agree with each other, as one moves to closer separations they start to diverge. This is to be expected since the $J - J_{\text{irr}}$ angular momentum contains negative terms (1.5 PN) related to the spin orbit coupling [46].

IV. MODIFIED SPIN FORMULATION

Motivated by the circulation expression for single stars and corotating binaries (27), we investigate a modification for the decomposition (15) proposed by Tichy [24]; i.e. we take

$$\hat{u}_i := \gamma_i^\alpha h u_\alpha = D_i \Phi + h u^t s_i \quad (31)$$

but otherwise adopt the same assumptions. In doing so, the circulation of a spinning star in a binary will be

$$C = R_0 \oint_c h u^t \psi^4 \delta_{ij} \hat{\Omega}_s \hat{\phi}_s^i d\hat{x}^j, \quad (32)$$

which apart from the coordinate terms (due to shift β^i) closely matches Eq. (27) of the circulation of a single rotating star. Now, the velocity with respect to the corotating frame becomes

$$V^i = \frac{D^i \Phi}{h u^t} - (\omega^i - s^i), \quad (33)$$

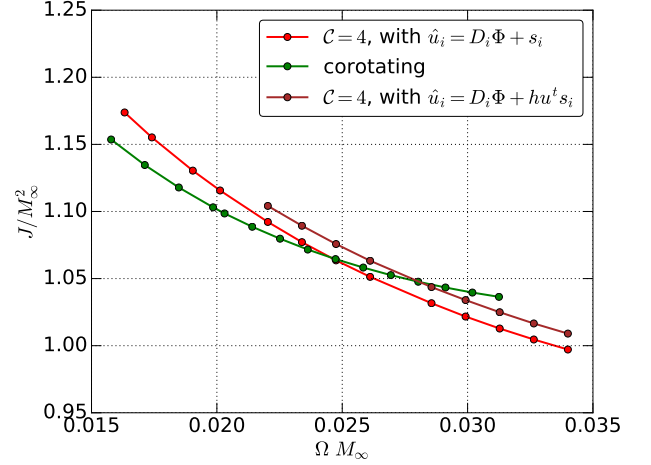


FIG. 6. Angular momentum curve for a binary system with constant circulation $C = 4$ and rest mass $M_0 = 1.5$, using decomposition (31), along with the same sequence as presented in Fig. 4, which uses the original decomposition Eq. (15). Also shown is the corotating sequence.

which can be thought as the same with the irrotational case and a replace

$$\omega^i \longleftrightarrow \omega^i - s^i, \quad (34)$$

where again here $\omega^i = \beta^i + \Omega \phi^i$ is the corotating shift. The Euler first integral now becomes

$$h^2 + D_i \Phi D^i \Phi = \lambda h u^t \quad (35)$$

where $\lambda := C + (\omega^i - s^i) D_i \Phi$. It turns out now that the equations are simplified and the relative quantities can be computed through a linear equation in $h u^t$,

$$h u^t = \frac{\lambda + 2s^i D_i \Phi}{\alpha^2 - s_i s^i}. \quad (36)$$

The denominator in the expression above is larger than zero, since even for very compact stars $\alpha^2 > 0.1$, which is approximately 1 order of magnitude larger than the square of the spin magnitude. Once $h u^t$ is computed from Eq. (36), the enthalpy is calculated from Eq. (35).

The velocity potential is determined from the conservation of rest mass,

$$\begin{aligned} \nabla^2 \Phi = & -\frac{2}{\psi} \partial^i \psi \partial_i \Phi + \psi^4 \partial_i [h u^t (\omega^i - s^i)] \\ & + 6 h u^t \psi^3 (\omega^i - s^i) \partial_i \psi \\ & - \partial_i \ln \left(\frac{\alpha \phi}{h} \right) [\partial^i \Phi - \psi^4 h u^t (\omega^i - s^i)] \end{aligned} \quad (37)$$

with boundary condition

$$\{[-\partial^i \Phi + \psi^4 h u^t (\omega^i - s^i)] \partial_i \rho\}_{\text{surface}} = 0. \quad (38)$$

In Fig. 6, we plot a sequence of constant rest mass $M_0 = 1.5$ and constant circulation $\mathcal{C} = 4$ using decomposition (31) along with the same sequence using the original decomposition (15) that we plotted in Fig. 4. We also show the corotating sequence for comparison. It is evident that the way one decomposes the velocity \hat{u}_i introduces an arbitrariness in the circulation, which in the present case results in a higher angular momentum for the system. This is not difficult to explain since the parabolic functional form of the hu^t factor in Eq. (31) results in a differentially rotating BNS, which increases the angular momentum of the system. On the other hand, this differential rotation, which naturally results from Eq. (31), can be canceled or modified by an appropriate choice of the input vector s^i , which must have a varying parameter Ω_s . Since spinning BNSs are expected to have a rotation law which is close to rigid rotation, decomposition (15) is closer to astrophysical expectations over (31). The latter can still produce almost uniformly rotating objects, but the spin input vector s_i is nontrivial.

V. DISCUSSION

Dynamical evolution of isentropic fluids conserves the baryon mass, entropy, and vorticity. Therefore, along with the rest mass, one can use the circulation of a neutron star to compute realistic sequences of binary neutron stars and measure their individual spin. In this paper, we extended our COCAL code to compute such equilibria and used it to make a critical assessment of various spin measures for BNS, as well as a connection with the spin of single rotating stars.

By computing sequences of constant angular momentum J , angular velocity, circulation, and dimensionless spin J/M^2 for single axisymmetric stars, we showed that in general all such family curves are distinct. For small spins, though, curves of constant circulation “run parallel” to those of constant J/M^2 ; therefore, conservation of circulation implies conservation of J/M^2 and vice versa. Using the approximation of conformal flatness and maximal slicing (which is typically used for BNS calculations), the angular momentum J equals the quasilocal spin J_{ql} , which is widely used to measure the angular momentum of a compact body in a binary scenario. For BNSs, neighboring equilibria satisfy the first law of thermodynamics by Friedman *et al.* and by computing sequences of constant rest mass and circulation, we show that the dimensionless spin is also approximately conserved at least for low spin binaries.

Motivated by the expression of circulation in single rotating stars, we explored an alternative decomposition for the 4-velocity than the one originally proposed by Tichy, which naturally led to differentially rotating binary systems, and discussed a potential ambiguity that results from any such decomposition.

Acknowledgments.—This work was supported by NSF Grants No. PHY-1602536 and No. PHY-1662211 and NASA Grant No. 80NSSC17K0070 to the University of Illinois at Urbana-Champaign as well as by a JSPS Grant-in-Aid for Scientific Research (C), Grants No. 15K05085 and No.

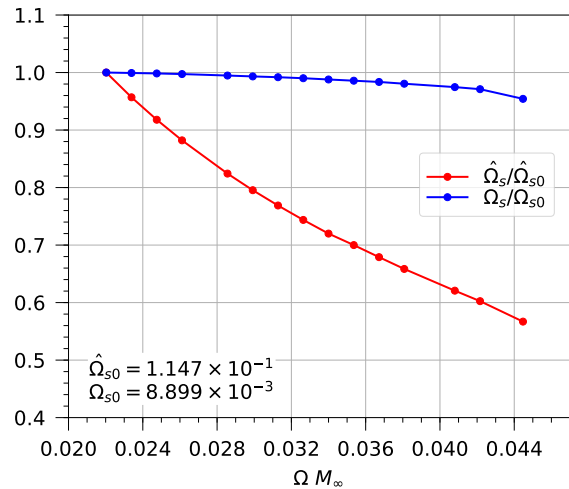


FIG. 7. Spin parameter Ω_s and the normalized parameter $\hat{\Omega}_s$ along the constant circulation $\mathcal{C} = 4$ and the constant rest mass $M_0 = 1.5$ sequence of Fig. 4.

18K03624, to the University of Ryukyus.

Appendix: Spin parameter Ω_s along a constant circulation and rest-mass sequence

In Fig. 7, we plot the spin parameter, both the original Ω_s and the normalized one $\hat{\Omega}_s$, for the $\mathcal{C} = 4$ sequence. To a high degree, a constant circulation sequence corresponds to a constant spinning parameter Ω_s for widely separated binaries [see Eq. (16)], but the normalized parameter $\hat{\Omega}_s$, which is used in our code, varies considerably along the sequence. Along a constant circulation sequence the maximum variation of Ω_s happens at the ISCO and is $\sim 4\%$. Having said that, we must keep in mind that Fig. 7 corresponds to $\mathcal{C} = 4$ or according to Fig. 5 quasilocal spin of ~ 0.17 . For high enough spins (> 0.5), this behavior may not be true. Also, if for the spin vector s^i , Eq. (16), one uses a more complicated expression (for example with multiple parameters), the behavior can change analogously. For the new sequence plotted in Fig. 6 using decomposition Eq. (31), the variation of Ω_s is twice of that of Fig. 7 using Eq. (15). In other words, the decomposition (15) introduces an arbitrariness to \hat{u}_i through the input spin vector s^i , which is necessary for computing the circulation. In a realistic scenario, any given spinning BNS has a particular \hat{u}_i , which is the result of hydrostatic equilibrium and its evolutionary history, and this determines its circulation. Targeting the circulation alone does not uniquely specify the velocity profile in the configuration. Hence, we can construct two sequences with the same circulation, one with a constant and the other with differential angular velocity, as we have seen in the last section above.

-
- [1] B. P. Abbott *et al.*, *Phys. Rev. Lett.* **119**, 161101 (2017), [arXiv:1710.05832 \[gr-qc\]](#).
- [2] A. Goldstein *et al.*, *The Astrophys. J. Lett.* **848**, L14 (2017).
- [3] V. Savchenko *et al.*, *Astrophys. J.* **848**, L15 (2017), [arXiv:1710.05449 \[astro-ph.HE\]](#).
- [4] J. W. T. Hessels, S. M. Ransom, I. H. Stairs, P. C. C. Freire, V. M. Kaspi, and F. Camilo, *Science* **311**, 1901 (2006), [astro-ph/0601337](#).
- [5] T. M. Tauris *et al.*, *Astrophys. J.* **846**, 170 (2017), [arXiv:1706.09438 \[astro-ph.HE\]](#).
- [6] X. Zhu, E. Thrane, S. Osłowski, Y. Levin, and P. D. Lasky, (2017), [arXiv:1711.09226 \[astro-ph.HE\]](#).
- [7] K. Stovall *et al.*, *Astrophys. J.* **854**, L22 (2018), [arXiv:1802.01707 \[astro-ph.HE\]](#).
- [8] A. D. Cameron *et al.*, *Mon. Not. R. Astron. Soc.* **475**, L57 (2018), [arXiv:1711.07697 \[astro-ph.HE\]](#).
- [9] M. Kramer *et al.*, *Science* **314**, 97 (2006), [arXiv:astro-ph/0609417 \[astro-ph\]](#).
- [10] T. W. Baumgarte, G. B. Cook, M. A. Scheel, S. L. Shapiro, and S. A. Teukolsky, *Phys. Rev. Lett.* **79**, 1182 (1997), [arXiv:gr-qc/9704024](#).
- [11] T. W. Baumgarte, G. B. Cook, M. A. Scheel, S. L. Shapiro, and S. A. Teukolsky, *Phys. Rev. D* **57**, 7299 (1998), [arXiv:gr-qc/9709026](#).
- [12] P. Marronetti, G. J. Mathews, and J. R. Wilson, *Phys. Rev. D* **58**, 107503 (1998), [arXiv:gr-qc/9803093](#).
- [13] L. Bildsten and C. Cutler, *Astrophys. J.* **400**, 175 (1992).
- [14] C. S. Kochanek, *Astrophys. J.* **398**, 234 (1992).
- [15] S. Bonazzola, E. Gourgoulhon, and J.-A. Marck, *Phys. Rev. Lett.* **82**, 892 (1999), [arXiv:gr-qc/9810072](#).
- [16] E. Gourgoulhon, P. Grandclément, K. Taniguchi, J.-A. Marck, and S. Bonazzola, *Phys. Rev. D* **63**, 064029 (2001), [arXiv:gr-qc/0007028](#).
- [17] P. Marronetti, G. J. Mathews, and J. R. Wilson, *Nucl. Phys. B* **80**, 07/14 (2000), [arXiv:gr-qc/9903105](#).
- [18] P. Marronetti, G. J. Mathews, and J. R. Wilson, *Phys. Rev. D* **60**, 087301 (1999), [arXiv:gr-qc/9906088](#).
- [19] K. Uryū and Y. Eriguchi, *Phys. Rev. D* **61**, 124023 (2000), [arXiv:gr-qc/9908059](#).
- [20] K. Uryū, M. Shibata, and Y. Eriguchi, *Phys. Rev. D* **62**, 104015 (2000), [arXiv:gr-qc/0007042](#).
- [21] P. Marronetti and S. L. Shapiro, *Phys. Rev. D* **68**, 104024 (2003), [arXiv:gr-qc/0306075 \[gr-qc\]](#).
- [22] T. W. Baumgarte and S. L. Shapiro, *Phys. Rev. D* **80**, 064009 (2009), [arXiv:0909.0952](#).
- [23] T. W. Baumgarte and S. L. Shapiro, *Phys. Rev. D* **80**, 089901 (2009).
- [24] W. Tichy, *Phys. Rev. D* **84**, 024041 (2011), [arXiv:1107.1440 \[gr-qc\]](#).
- [25] W. Tichy, *Phys. Rev. D* **86**, 064024 (2012), [arXiv:1209.5336](#).
- [26] P. Tsatsin and P. Marronetti, *Phys. Rev. D* **88**, 064060 (2013), [arXiv:1303.6692](#).
- [27] K. Uryū and A. Tsokaros, *Phys. Rev. D* **85**, 064014 (2012), [arXiv:1108.3065 \[gr-qc\]](#).
- [28] A. Tsokaros, K. Uryū, and L. Rezzolla, *Phys. Rev. D* **91**, 104030 (2015), [arXiv:1502.05674 \[gr-qc\]](#).
- [29] A. Tsokaros, B. C. Mundim, F. Galeazzi, L. Rezzolla, and K. Uryū, *Phys. Rev. D* **94**, 044049 (2016), [arXiv:1605.07205 \[gr-qc\]](#).
- [30] S. Bernuzzi, T. Dietrich, W. Tichy, and B. Brgmann, *Phys. Rev. D* **89**, 104021 (2014), [arXiv:1311.4443 \[gr-qc\]](#).
- [31] T. Dietrich, N. Moldenhauer, N. K. Johnson-McDaniel, S. Bernuzzi, C. M. Markakis, B. Brgmann, and W. Tichy, *Phys. Rev. D* **92**, 124007 (2015), [arXiv:1507.07100 \[gr-qc\]](#).
- [32] N. Tacik *et al.*, *Phys. Rev. D* **92**, 124012 (2015), [Erratum: *Phys. Rev. D* 94, no.4, 049903 (2016)], [arXiv:1508.06986 \[gr-qc\]](#).
- [33] J. L. Friedman, K. Uryū, and M. Shibata, *Phys. Rev. D* **65**, 064035 (2002), [Erratum: *Phys. Rev. D* 70, 129904 (2004)], [arXiv:gr-qc/0108070 \[gr-qc\]](#).
- [34] J. L. Friedman and N. Stergioulas, *Rotating Relativistic Stars*, Cambridge Monographs on Mathematical Physics (Cambridge University Press, 2013).
- [35] K. Uryū, A. Tsokaros, F. Galeazzi, H. Hotta, M. Sugimura, K. Taniguchi, and S. Yoshida, *Phys. Rev. D* **93**, 044056 (2016).
- [36] T. W. Baumgarte and S. L. Shapiro, *Numerical Relativity: Solving Einstein's Equations on the Computer* (Cambridge University Press, 2010).
- [37] L. Rezzolla and O. Zanotti, *Relativistic Hydrodynamics* (Oxford University Press, Oxford, UK, 2013).
- [38] S. Bonazzola, E. Gourgoulhon, and J.-A. Marck, *Phys. Rev. D* **56**, 7740 (1997), [arXiv:gr-qc/9710031](#).
- [39] H. Asada, *Phys. Rev. D* **57**, 7292 (1998), [arXiv:gr-qc/9804003](#).
- [40] M. Shibata, *Phys. Rev. D* **58**, 024012 (1998), [arXiv:gr-qc/9803085 \[gr-qc\]](#).
- [41] S. A. Teukolsky, *Astrophys. J.* **504**, 442 (1998), [arXiv:gr-qc/9803082 \[gr-qc\]](#).
- [42] K. Uryū, A. Tsokaros, L. Baiotti, F. Galeazzi, N. Sugiyama, K. Taniguchi, and S. Yoshida, *Phys. Rev. D* **94**, 101302 (2016), [arXiv:1606.04604 \[astro-ph.HE\]](#).
- [43] M. Alford, M. Braby, M. Paris, and S. Reddy, *Astrophys. J.* **629**, 969 (2005), [arXiv:nucl-th/0411016 \[nucl-th\]](#).
- [44] J. S. Read, B. D. Lackey, B. J. Owen, and J. L. Friedman, *Phys. Rev. D* **79**, 124032 (2009).
- [45] T. Dietrich, S. Bernuzzi, M. Ujevic, and W. Tichy, *Phys. Rev. D* **95**, 044045 (2017), [arXiv:1611.07367 \[gr-qc\]](#).
- [46] L. Blanchet, *Living Reviews in Relativity* **17**, 2 (2014), [arXiv:1310.1528 \[gr-qc\]](#).